

Brief paper

Plasma vertical stabilization with actuation constraints in the DIII-D tokamak[☆]

E. Schuster^{a,*}, M.L. Walker^b, D.A. Humphreys^b, M. Krstić^c

^a*Mechanical Engineering and Mechanics, Lehigh University, 19 Memorial Drive West, Bethlehem, PA 18015-3085, USA*

^b*General Atomics, P.O. Box 85608, San Diego, CA 92186-5608, USA*

^c*Mechanical and Aerospace Engineering, University of California at San Diego, 9500 Gilman Dr., La Jolla, CA 92093-0411, USA*

Received 12 March 2004; received in revised form 23 October 2004; accepted 3 December 2004

Available online 25 April 2005

Abstract

In the advanced tokamak (AT) operating mode of the DIII-D tokamak, an integrated multivariable controller takes into account highly coupled influences of plasma equilibrium shape, profile, and stability control. Time-scale separation in the system allows a multi-loop design: the inner loop closed by the nominal vertical controller designed to control a linear exponentially unstable plant and the outer loop closed by the nominal shape controller designed to control a linear stabilized plant. Due to actuator constraints, the nominal vertical controller fails to stabilize the vertical position of the plasma inside the tokamak when large or fast disturbances are present or when the references coming from the shape controller change suddenly. Anti-windup synthesis is proposed in this paper to find a nonlinear modification of the nominal vertical controller that prevents vertical instability and undesirable oscillations but leaves the inner loop unmodified when there is no input saturation.

© 2005 Elsevier Ltd. All rights reserved.

Keywords: Nuclear fusion; Tokamaks; Plasma vertical stabilization; Actuator saturation; Anti-windup augmentation

1. Introduction

Demands for more varied shapes of the plasma and requirements for high performance regulation of the plasma boundary and internal profiles are the common denominator of the advanced tokamak (AT) operating mode in DIII-D (Luxon, 2002). This operating mode requires multivariable control techniques (Walker et al., 2003) to take into account the highly coupled influences of equilibrium shape, profile,

and stability control. The initial step toward integrating multiple individual controls is implementation of a multivariable shape and vertical controller for routine operational use which can be integrated in the long term with control of plasma profiles such as pressure, radial E-field, and current profiles.

The problem of vertical and shape control in tokamaks was and is still extensively studied in the fusion community. A recent summary of the existing work in the field can be found in Albanese and Ambrosino (2000). Several solutions for the design of the nominal controller were proposed for different tokamaks using varied control techniques based on linearized models. Although the saturation of coil currents and voltages (actuators) is a common problem in tokamaks and there were efforts to minimize the control demand for shape and vertical control and to avoid saturation (Ambrosino, Ariola, Pironti, Portone, & Walker, 2001), the saturation of the actuators was rarely taken into account in the design of the controllers until recently

[☆] This paper was not presented at any IFAC meeting. This paper was recommended for publication in revised form by Associate Editor T. A. Johansen under the direction of Editor F. Allgower. This work was supported in part by grants from UCEI and NSF and by DoE contract number DE-AC03-99ER54463.

* Corresponding author.

E-mail addresses: schuster@lehigh.edu (E. Schuster), walker@fusion.gat.com (M.L. Walker), dave.humphreys@gat.com (D.A. Humphreys), krstic@ucsd.edu (M. Krstić).

(Scibile & Kouvaritakis, 2001; Favez, Mullhaupt, Srinivasan, Lister, & Bonvin, 2003). Although similar in concept, our work uses a different approach to the problem: anti-windup compensator. The input constraints are not taken into account at the moment of designing the nominal controller. The goal is not the design of the nominal controller but the design of an anti-windup compensator that blends any given nominal controller, which is designed to fulfill some local (saturation is not considered) performance criterion, with a nonlinear feedback designed to guarantee stability in the presence of input saturation but not necessarily tuned for local performance.

The paper is organized as follows. Section 2 introduces the strategy proposed for plasma shape and vertical position control in the DIII-D tokamak. Section 3 introduces the basics of the anti-windup method. The characteristics of our plant and its controllable region are presented in Section 4. The design of the anti-windup compensator is presented in Section 5. Some implementation issues are discussed in the same section. Finally, the conclusions are presented in Section 6.

2. Control Strategy

Time-scale separation of vertical and shape control appears to be critical for DIII-D, since multivariable shape controllers can require significant computation. Fig. 1 shows the closed-loop system comprised of the DIII-D plant and stabilizing vertical controller. This system is stable and the 6 coil currents F2A, F2B, F6A, F6B, F7A, and F7B are approximately controlled to a set of input reference values. As a result, this system can act as an inner control loop for shape control.

The problem of highly nonlinear outer power supplies (choppers) was addressed previously by constructing closed-loop controllers using a nonlinear output inversion. However, this solution, for the outer loop, is not fast enough to

be implemented in the inner loop. A possible approach to deal with the inner choppers is shown in Fig. 1. To take into account the nonlinear nature of the choppers, we now incorporate them into an augmented saturation block. The nominal linear vertical controller is synthesized without using a model of the choppers and its output y_c is equal to the coil voltages in the absence of saturation. A chopper inverse function, which is part of the vertical controller, computes the necessary command voltages V_c within the saturation levels to make u equal to y_c . When $|y_c|$ is large, the saturation block will obviously result in $|u|$ being smaller than $|y_c|$. Although the saturation levels of the command voltages V_c are still fixed values (± 10 V), the saturation levels of the augmented saturation block are functions of time, i.e., of the coil load currents I_L and DC charging supply voltage V_{ps} .

To make this approach successful, the inner controller (vertical controller, Fig. 1) must guarantee stability of the plant for all commands coming from the outer controller (shape controller, Fig. 1). However, the constraints on the input of the inner plant due to the saturation of the actuators may prevent this goal from being achieved. The saturation of the coil voltages cannot only degrade the performance of the inner closed-loop system but also impede the vertical stabilization when the synthesis of the nominal inner controller does not account for plant input saturation. The inner loop design must take care then of the windup of that loop and ensure vertical stability for any command coming from the outer controller. We understand as windup the phenomenon characterized by degradation of nominal performance and even loss of stability due to magnitude and/or rate limits in the control actuation devices. The anti-windup synthesis problem is to find a nonlinear modification of the predesigned nominal linear controller that prevents vertical instability and undesirable oscillations (keeping the nominal controller well-behaved) but leaves the nominal closed loop unmodified when there is no input saturation. This problem is different from the problem of synthesizing a controller that accounts for input saturation without requiring it to match a given predesigned arbitrary controller locally. Several survey papers (Hanus, 1988; Åström & Rundqwist, 1989; Morari, 1993) describe early ad-hoc anti-windup methods. Recently several other approaches have been proposed (Gilbert & Kolmanovsky, 1999; Bemporad & Morari, 1999; Zheng, Kothare, & Morari, 1994; Scibile & Kouvaritakis, 2000; Shamma, 2000; Mulder, Kothare, & Morari, 2001; Miyamoto & Vinnicombe, 1996). Due to the characteristics of our problem we follow the ideas discussed in Teel (1999) for exponentially unstable linear systems.

3. Anti-windup compensator fundamentals

We consider exponentially unstable linear plants with control input $u \in \mathcal{R}^m$ and measurements $y \in \mathcal{R}^p$. We write the model of our system in state-space form, $\dot{x} = Ax + Bu$, separating the stable modes ($x_s \in \mathcal{R}^{n_s}$) from the exponentially

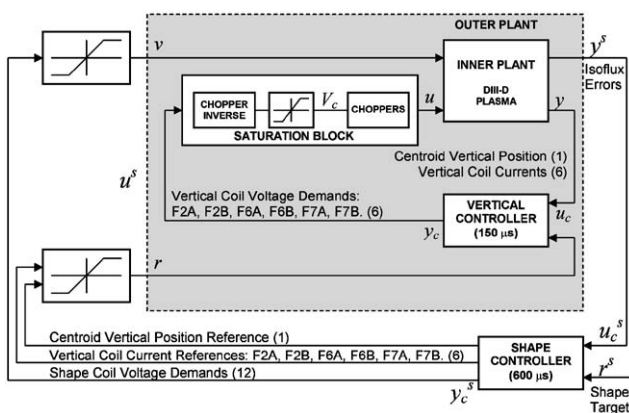


Fig. 1. Plant Architecture.

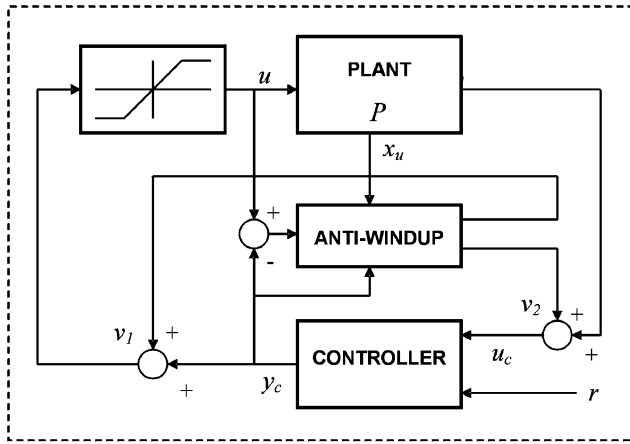


Fig. 2. Anti-windup scheme.

unstable modes ($x_u \in \mathfrak{R}^{n_u}$),

$$\dot{x} = \begin{bmatrix} \dot{x}_s \\ \dot{x}_u \end{bmatrix} = \begin{bmatrix} A_s & A_{su} \\ 0 & A_u \end{bmatrix} \begin{bmatrix} x_s \\ x_u \end{bmatrix} + \begin{bmatrix} B_s \\ B_u \end{bmatrix} u, \quad (1)$$

$$y = Cx + Du, \quad (2)$$

where the dimension of the state vector x is $n = n_s + n_u$. The eigenvalues of A_s have non-positive real part, and the eigenvalues of A_u have positive real part. In addition, we consider that a nominal controller with state $x_c \in \mathfrak{R}^{n_c}$, input $u_c \in \mathfrak{R}^p$, output $y_c \in \mathfrak{R}^m$ and reference $r \in \mathfrak{R}^p$, has been already designed so that the closed loop system with interconnection conditions $u = y_c$, $u_c = y$, is well posed and internally stable. When the controller output is subject to saturation, i.e., the interconnection conditions are changed to $u = \text{sat}(y_c)$, $u_c = y$, the synthesis of an anti-windup scheme is necessary. In this case the interconnection conditions are modified to

$$u = \text{sat}(y_c + v_1), \quad u_c = y + v_2, \quad (3)$$

where the signals v_1 and v_2 are the outputs of the anti-windup compensator (Teel, 1999)

$$\dot{x}_{aw} = Ax_{aw} + B[\text{sat}(y_c + v_1) - y_c], \quad (4)$$

$$v_1 = (\beta(x_u) - 1)y_c + \alpha(x_u - \beta(x_u)(x_u - x_{aw_u}), \beta(x_u)\kappa(x_{aw})), \quad (5)$$

$$v_2 = -Cx_{aw} - D[\text{sat}(y_c + v_1) - y_c], \quad (6)$$

and where the anti-windup state x_{aw} is also divided into stable (x_{aw_s}) and unstable (x_{aw_u}) modes.

The anti-windup scheme is illustrated in Fig. 2. In addition to modifying the nominal controller when input saturation is encountered, the anti-windup compensator modifies the closed loop if the exponentially unstable modes get close to the boundary of some reasonably large subset of the region where these unstable modes are controllable with the given bound on the control (controllable region). The “distance” from this boundary is measured by the function β ,

defined as

$$\beta(x_u) = \begin{cases} 1, & x_u \in \chi_{\text{lower}}, \\ 0, & x_u \notin \chi_{\text{upper}} \end{cases} \quad (7)$$

and interpolated in between, where $\chi_{\text{lower}} \subset \chi_{\text{upper}}$ are subsets of χ , the domain of attraction of the disturbance-free system subject to the saturation of the output controller or what we call controllable region. The anti-windup approach requires that the states move in a region χ_{upper} that is smaller than the controllable region χ . The freedom to define χ_{lower} and χ_{upper} is a tool the designer has to deal with the disturbances that although not modeled are present in the system. The smaller χ_{lower} and χ_{upper} , the bigger the disturbances tolerated by the system without escaping the controllable region χ . When the unstable modes get close to the boundary of the controllable region χ , the closed loop is modified by the function α , which takes over control of the plant ($\beta = 0 \Rightarrow v_1 = -y_c + \alpha \Rightarrow u = \text{sat}(\alpha)$). One choice of the function $\alpha : \mathfrak{R}^{n_u} \times \mathfrak{R}^m \rightarrow \mathfrak{R}^m$ is given by (Teel, 1999)

$$\alpha(\zeta, \omega) = K_u \zeta + \omega, \quad (8)$$

where K_u is such that $A_u + B_u K_u$ is Hurwitz. The function $\kappa(x_{aw})$ can be designed to improve the performance of the antiwindup scheme when the controller output is not saturating. However, in this work we will introduce a different approach toward the same goal. It is important to note that this scheme requires the measurement or estimation of the exponentially unstable modes x_u .

4. Plant model

Fig. 1 illustrates the architecture of our plant. The dynamics of the inner plant can be written as

$$\begin{aligned} \dot{x} &= Ax + Bu + Ev, \\ y &= Cx + Du + Gv, \end{aligned} \quad (9)$$

where there are $n \approx 50$ states. Separating the stable modes ($x_s \in \mathfrak{R}^{n_s}$) from the exponentially unstable modes ($x_u \in \mathfrak{R}^{n_u}$), we can write

$$\begin{bmatrix} \dot{x}_s \\ \dot{x}_u \end{bmatrix} = \begin{bmatrix} A_s & A_{su} \\ 0 & A_u \end{bmatrix} \begin{bmatrix} x_s \\ x_u \end{bmatrix} + \begin{bmatrix} B_s \\ B_u \end{bmatrix} u + \begin{bmatrix} E_s \\ E_u \end{bmatrix} v. \quad (10)$$

The vector u of dimension $m=6$ are the voltage commands for power supplies on the vertical coils F2A, F2B, F6A, F6B, F7A and F7B, the vector v of dimension $q \leq 12$ are the voltage demands for the shape coils, the vector y of dimension $p = 7$ consists of the six vertical coil currents I_L and the plasma centroid (center of mass of plasma current) position. Due to the composition of the output vector y it is convenient to write the reference for the nominal controller as $r = [r_I^T \ r_Z]^T$, where r_I are the current references for the six vertical coils and r_Z is the centroid position reference. The main characteristics of our plant can be summarized

as: (1) There is only one unstable eigenvalue, i.e., $n_u = 1$. The $n_s = n - 1$ stable eigenvalues all have strictly negative real parts. However, some of them are very close to zero (slow modes). (2) Defining the saturation function

$$\text{sat}_{a^{\min}}^{a^{\max}}(b) = \begin{cases} a^{\max} & \text{if } a^{\max} < b, \\ b & \text{if } a^{\min} \leq b \leq a^{\max}, \\ a^{\min} & \text{if } b < a^{\min}, \end{cases} \quad (11)$$

the saturation of the channel i of the controller, for $i = 1, \dots, m$, will be denoted as

$$\text{sat}(y_{c_i}) = \text{sat}_{M_i^{\min}(t)}^{M_i^{\max}(t)}(y_{c_i}),$$

where the saturation levels $M_i^{\min}(t)$ and $M_i^{\max}(t)$ are functions of time (i.e., of coil load current $I_L(t)$ and DC supply voltage $V_{ps}(t)$). (3) There is no direct measurement of the unstable mode x_u . (4) The control input u is not the only input of the inner plant. In addition to the voltage commands u for the vertical coil from the vertical controller, there are voltage demands v for the shape coils coming from the shape controller.

Given the dynamics of the unstable mode ($\dot{x}_u = A_u x_u + B_u u + E_u v$) in (10), we can compute the minimum and maximum values of the unstable mode that can be reached without losing control authority to stabilize the system,

$$x_u^{\max} = \frac{-(B_u u)^{\min} - E_u v}{A_u}, \quad (12)$$

$$x_u^{\min} = \frac{-(B_u u)^{\max} - E_u v}{A_u}, \quad (13)$$

and define the controllable region as

$$\chi = \{x \in \mathfrak{R}^n : x_u^{\min} \leq x_u \leq x_u^{\max}\}. \quad (14)$$

The maximal and minimal control are given by

$$(B_u u)^{\min} = \sum_{i=1}^m B_{u_i} g_i(-B_{u_i}), \quad (15)$$

$$(B_u u)^{\max} = \sum_{i=1}^m B_{u_i} g_i(B_{u_i}), \quad (16)$$

where B_{u_i} is the i th component of B_u and $g_i(a) = M_i^{\max}$ if $a > 0$, $g_i(a) = M_i^{\min}$ if $a < 0$.

The controllable region is the state space region where there exists an input u within the saturation limits that can steer the system to the origin. The definition of x_u^{\max} in (12) implies that we can make $\dot{x}_u < 0$ for all $0 < x_u < x_u^{\max}$ by taking $B_u u = (B_u u)^{\min}$. In similar way, the definition of x_u^{\min} in (13) implies that we can make $\dot{x}_u > 0$ for all $x_u^{\min} < x_u < 0$ by taking $B_u u = (B_u u)^{\max}$.

5. Anti-windup design

5.1. Design of function β

Once χ is determined, we can define

$$\chi_{\text{lower}} = \{x \in \mathfrak{R}^n : x_u^{\min,l} < x_u < x_u^{\max,l}\}, \quad (17)$$

$$\chi_{\text{upper}} = \{x \in \mathfrak{R}^n : x_u^{\min,u} < x_u < x_u^{\max,u}\}, \quad (18)$$

where $x_u^{\min,l} = f^l x_u^{\min}$, $x_u^{\max,l} = f^l x_u^{\max}$, $x_u^{\min,u} = f^u x_u^{\min}$, $x_u^{\max,u} = f^u x_u^{\max}$, and $0 < f^l < f^u < 1$. Once χ , χ_{lower} and χ_{upper} are defined ($\chi_{\text{lower}} \subset \chi_{\text{upper}} \subset \chi$), the function β is defined according to (7).

5.2. Design of gain K_u

The feedback gain K_u in (8) is designed such that

$$A_u + B_u K_u < 0, \quad (19)$$

$$\text{sgn}(B_{u_i}) = -\text{sgn}(K_{u_i}), \quad (20)$$

$$|K_{u_i} x_u^{\max,u}| > \max(|M_i^{\min}|, |M_i^{\max}|), \quad (21)$$

$$|K_{u_i} x_u^{\min,u}| > \max(|M_i^{\min}|, |M_i^{\max}|), \quad (22)$$

for $i = 1, \dots, m$, where B_{u_i} and K_{u_i} are the i th components of B_u and K_u respectively. With (21) and (22), we guarantee that for $x_u^{\max,u} \leq x_u < x_u^{\max}$ (where $\beta(x_u) = 0$) we have $B_u u = B_u \text{sat}(K_u x_u) = (B_u u)^{\min}$, and consequently that

$$\begin{aligned} \text{sgn}(\dot{x}_u) &= \text{sgn}(A_u x_u + B_u \text{sat}(K_u x_u) + E_u v) \\ &= \text{sgn}(A_u x_u + (B_u u)^{\min} + E_u v) < 0 \end{aligned} \quad (23)$$

by definition (12). In similar way we can show that for $x_u^{\min} \leq x_u < x_u^{\min,u}$ (where $\beta(x_u) = 0$) we have

$$\text{sgn}(\dot{x}_u) > 0. \quad (24)$$

Conditions (23) and (24) ensure stabilization of the unstable mode when $\beta(x_u) = 0$ through the signal $v_1 = -y_c + K_u x_u$.

5.3. Design of the function κ

We want to make the states x_{aw} of the anti-windup compensator converge to zero as fast as possible when the unstable mode is in the “safe” region, defined by the condition $\beta(x_u) = 1$, and no channel of the controller output is saturating. The function $\kappa(x_{aw})$ in (5) can be designed toward this goal. However, at this point we depart from the original method and follow an alternative procedure for simplicity and effectiveness. We make $\kappa(x_{aw}) = 0$ and modify the structure of the anti-windup compensator (4) as follows:

$$\begin{aligned} \dot{x}_{aw} &= A x_{aw} + B[\text{sat}(y_c + v_1) - y_c] \\ &\quad - [1 - \gamma(y_c + v_1)]\delta x_{aw}, \quad \delta > 0, \end{aligned} \quad (25)$$

where the function $\gamma = \max(\gamma_1, \gamma_2, \dots, \gamma_m)$ is an indication of saturation, being zero if none of the input channel

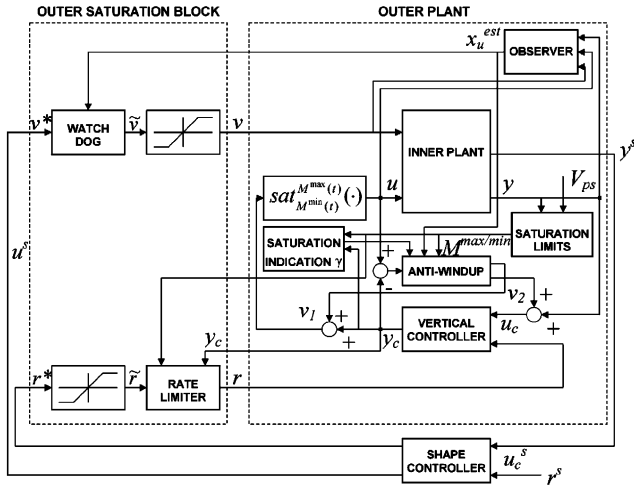


Fig. 3. Inner loop anti-windup scheme.

is saturating and one otherwise. The function γ_i , defined for each channel i , becomes one when the signal coming from the controller and anti-windup goes above M_i^{max} or below M_i^{min} . However, the function γ_i recovers its zero value only when the signal coming from the controller and anti-windup becomes lower than $M_i^{max,\gamma} < M_i^{max}$ or higher than $M_i^{min,\gamma} > M_i^{min}$. These hysteresis loops are introduced to avoid chattering in the scheme. In this way, when the unstable mode is in the “safe” region and there is no saturation, the dynamics of the anti-windup can be written as

$$\begin{aligned} \dot{x}_{aw} &= Ax_{aw} + Bv_1 - \delta x_{aw} \\ &= \begin{bmatrix} A_s - \delta I_s & A_{su} + B_s K_u \\ 0 & A_u + B_u K_u - \delta I_u \end{bmatrix} \begin{bmatrix} x_{aw_s} \\ x_{aw_u} \end{bmatrix}, \end{aligned} \quad (26)$$

$$v_1 = K_u x_{aw_u}, \quad (27)$$

$$v_2 = -Cx_{aw} - Dv_1, \quad (28)$$

where I_s and I_u are identity matrices of appropriate dimension. The rate of convergence of x_{aw} to zero can be regulated now by the gain δ .

A scheme of the anti-windup design is shown in Fig. 3. The *Saturation Limits* block computes the saturation levels M_i^{min} and M_i^{max} , for $i = 1, \dots, m$, which are functions of time (i.e., of coil load currents $I_L(t)$ and DC supply voltage $V_{ps}(t)$). These saturation levels are used by the *Saturation Indication* and *Anti-Windup* blocks to compute the function γ and the controllable region χ respectively. The *Observer* block estimates the unstable mode which cannot be measured. This estimate is used by the *Anti-Windup* block to compute the function β . The *Saturation Indication* computes γ to speed up the convergence of slow modes (and v_2) to zero. Once the controllable region χ and the function β are computed, and the function γ provided, the *Anti-Windup* block is able to achieve stability through the signal v_1 and keep the nominal controller well-behaved through the signal v_2 . We are controlling the current in the vertical coils by modulating

their imposed voltages. There will be a minimum integration time constant which will depend on the inductance of the coils. Given a maximum coil voltage value dictated by the saturation level, we will have then a maximum rate of variation for the coil current. Any reference r_I (imposed by the shape controller) that exceeds this physical rate limit will only cause performance deterioration due to the windup of the controller. The *Rate Limiter* is designed to prevent the shape controller from asking the system for a response rate that cannot be physically fulfilled. As it is shown in Fig. 1 and stated in (9), our plant is also governed by the voltage demands for the shape coils v coming from the shape controller. This represents a potential risk of instability for our plant because the unstable mode can be potentially pushed outside the controllable region by shape control voltages. The goal of the *Watch-Dog* is to permanently monitor and regulate the value of the shape coil voltage demands to avoid the loss of controllability of the unstable mode due to the sudden shrinkage of the controllable region.

The stability of the anti-windup scheme is guaranteed when the unstable mode is directly measured (Teel, 1999). When there is no such direct measurement, a bad estimation of the unstable mode can prevent the anti-windup compensator to stabilize the system. A high gain observer is required in this case to ensure that the estimation is fast enough to prevent any excursion of the unstable mode outside the controllable region. The estimate \hat{x}_u is substituted for x_u in the anti-windup dynamics, which, summarizing (5), (6), (8), (25), is given by

$$\begin{aligned} \dot{x}_{aw} &= Ax_{aw} + B[\text{sat}(y_c + v_1) - y_c] \\ &\quad - [1 - \gamma(y_c + v_1)]\delta x_{aw}, \\ v_1 &= (\beta(\hat{x}_u) - 1)y_c + K_u[\hat{x}_u - \beta(\hat{x}_u)(\hat{x}_u - x_{aw_u})], \\ v_2 &= -Cx_{aw} - D[\text{sat}(y_c + v_1) - y_c]. \end{aligned} \quad (29)$$

For our simulation studies, a conventional Luenberger observer was implemented. However, during the implementation stage other types of observers more suitable for noisy environments will be considered. From the observer we do not need much accuracy, we only need to know if the unstable mode is inside χ_{lower} or outside χ_{upper} . Certain level of noise in the estimation can be tolerated because it is always possible to compensate the inaccuracy of the observer with a convenient selection (reduction) of the design parameters f^l and f^u , paying the price on the other hand of reducing conservatively the region χ_{upper} where we allow the states to move.

A performance comparison between the system without and with anti-windup can only be achieved when the changes in the current references are small enough to avoid instability in the system without anti-windup. In this case, the presence of the anti-windup compensator, which shows its effectiveness preventing instability for larger changes in the current references, must not degrade significantly the response of the system. Fig. 4 shows such comparison. The step

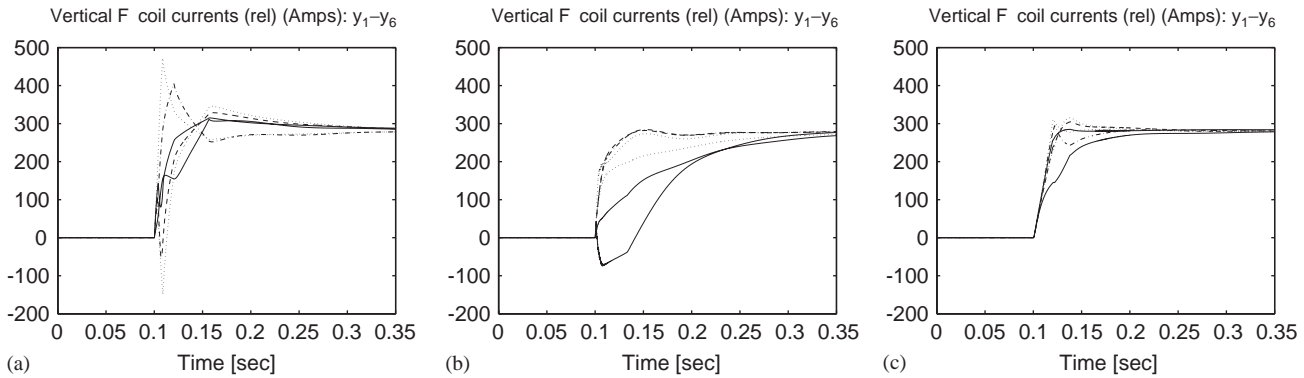


Fig. 4. System response with anti-windup and rate limiter to step changes of approximately 280 A in r_{I_i} , for $i = 1, \dots, m$, at $t = 0.1$ s ($r_Z = 0$ and $v = 0$). (a) No anti-windup, (b) anti-windup $\delta > 0$, (c) anti-windup $\delta > 0$ + rate limiter with variable rate limit.

response (b) is smoother and shows a settling time that is approximately the same as shown in the step response without anti-windup (a). The rate limiter in (c) not only makes the step response even smoother but also reduces the settling time considerably for some of the coils.

6. Conclusions

The proposed scheme has been shown in nonlinear simulations to be very effective in guaranteeing stability of the inner loop in the presence of voltage saturation of the vertical coils. The scheme is being implemented and will be tested in experimental conditions. After succeeding in the vertical stabilization of the plasma in experimental conditions, efforts will be concentrated on the design of the outer shape control loop. The necessity of a similar anti-windup scheme for the outer loop is anticipated; not only due to the inherent limitations of its actuators but also due to the fact that the inner loop will modify, through the watch-dog and rate limiter, the control signals of the outer loop in order to preserve stability of the inner plant and improve performance. In this case, we will deal with a stable (stabilized by the inner loop design) but nonlinear plant.

References

- Albanese, R., & Ambrosino, G. (2000). Current, position and shape control of tokamak plasmas: A literature review. *IEEE Conference on Decision and Control* (pp. 412–418).
- Ambrosino, G., Ariola, M., Pironti, A., Portone, A., & Walker, M. (2001). A control scheme to deal with coil current saturation in a tokamak. *IEEE Transactions on Control Systems Technology*, 9, 831–838.
- Åström, K. J., & Rundqwist, L. (1989). Integrator windup and how to avoid it. *American Control Conference* (pp. 1693–1698).
- Bemporad, A., & Morari, M. (1999). Control of systems integrating logic dynamics and constraints. *Automatica*, 35, 407–427.
- Favez, J.-Y., Mullhaupt, Ph., Srinivasan, B., Lister, J. B., & Bonvin, D. (2003). Improving the region of attraction of ITER in the presence of actuator saturation. *IEEE Conference on Decision and Control* (pp. 4616–4621).
- Gilbert, E. G., & Kolmanovsky, I. V. (1999). Set-point control of nonlinear systems with state and control constraints: A Lyapunov-function,

Reference-Governor approach. *IEEE Conference on Decision and Control* (pp. 2507–2512).

- Hanus, R. (1988). Antiwindup and bumpless transfer: A survey. *12th IMACS world congress* (pp. 59–65).
- Luxon, J. L. (2002). A design retrospective of the DIII-D tokamak. *Nuclear Fusion*, 42, 614–633.
- Miyamoto, A., & Vinnicombe, G. (1996). Robust control of plants with saturation nonlinearity based on coprime factor representation. *IEEE Conference on Decision and Control* (pp. 2838–2840).
- Morari, M. (1993). Essays on control: Perspectives in the theory and its applications. in: H. L., Trentelman, & J. C., Willems (Eds.), *Some control problems in the process industries* (pp. 55–77). Boston: Birkhauser.
- Mulder, E. F., Kothare, M. V., & Morari, M. (2001). Multivariable anti-windup controller synthesis using linear matrix inequalities. *Automatica*, 37, 1407–1416.
- Scibile, L., & Kouvaritakis, B. (2000). Stability region for a class of open-loop unstable linear systems: Theory and application. *Automatica*, 36, 37–44.
- Scibile, L., & Kouvaritakis, B. (2001). A discrete adaptive near-time optimum control for the plasma vertical position in a tokamak. *IEEE Transactions on Control Systems Technology*, 9, 148–162.
- Shamma, J. S. (2000). Anti-windup via constrained regulation with observers. *Systems and Control Letters*, 40, 1869–1883.
- Teel, A. R. (1999). Anti-Windup for exponentially unstable linear systems. *International Journal of Robust and Nonlinear Control*, 9, 701–716.
- Walker, M. L., Ferron, J. R., Humphreys, D. A., Johnson, R. D., Leuer, J. A., Penaflor, B. G., Pironti, A., Ariola, M., & Schuster, E. (2003). Next-generation plasma control in the DIII-D tokamak. *Fusion Engineering and Design*, 66–68, 749–753.
- Zheng, A., Kothare, M. V., & Morari, M. (1994). Anti-windup design for internal model control. *International Journal of Control*, 60, 1015–1024.



Eugenio Schuster holds undergraduate degrees in Electronic Engineering (Buenos Aires University, Argentina, 1993) and Nuclear Engineering (Balseiro Institute, Argentina, 1998). He obtained his M.Sc. (2000) and Ph.D. (2004) degrees in Mechanical & Aerospace Engineering from University of California San Diego and is currently Assistant Professor at Lehigh University. His research interests include the application of nonlinear control techniques

to complex physical systems such as fusion reactors, plasmas, magneto-hydrodynamic flows, and particle accelerators.



Michael Walker obtained his Ph.D. in Mathematics in 1992 from the University of California San Diego. He is currently employed at General Atomics in San Diego, where he provides control development support for the DIII-D tokamak and for several other tokamaks around the world. He is presently serving as a guest editor for an upcoming special issue of the IEEE Control Systems Magazine on tokamak plasma control.



Miroslav Krstić got his Ph.D. in 1994 from the University of California at Santa Barbara and is currently Professor at UC, San Diego. He is an IEEE Fellow and has received the NSF Career, ONR YI, and PECASE awards, as well as the Axelby and Schuck paper prizes. Krstic is a co-author of the books *Nonlinear and Adaptive Control Design* (1995), *Stabilization of Nonlinear Uncertain Systems* (1998), *Flow Control by Feedback* (2002), and *Real Time Optimization by Extremum Seeking Control* (2003).



Dr. David Humphreys received his Ph.D. in 1990 from the Massachusetts Institute of Technology and is currently head of the DIII-D Engineering Physics Group at General Atomics. His 20 years of experience in fusion plasma physics and control engineering have included engineering physics and MHD analysis for many operating and next-generation devices. He is the author of numerous technical publications, and is a member of the American Physical Society and the Sigma Xi Scientific Research Society.